Front. Energy 2022, 16(5): 700–705
https://doi.org/10.1007/s11708-022-0842-8

PERSPECTIVE

**Yanfang SONG, Xiao DONG, Wei CHEN, Wei WEI**

# Hollow-fiber gas penetration electrodes efficiently produce renewable synthetic fuels



Increasing $CO_2$ levels in the atmosphere due to the consumption of large amounts of fossil fuels is exacerbating global climate change, which seriously threatens sustainable human development. As a responsible and respectable country, China has announced remarkable goals of reaching a carbon emission peak and achieving carbon neutrality, which are challenging missions with enormous contributions to the world. As a strategic support, disruptive and transformative energy technologies are urgently required to develop new green and low-carbon energy industries. Renewable energy sources such as wind and sun, which can generate zero-carbon electric power, have been rapidly developed in recent years. In China, the cumulatively installed capacity of renewable clean energy power generation had reached 1.06 billion kW by the end of 2021, accounting for nearly 44.8% of the total installed capacity [1]. However, owing to the intrinsic inferiorities of instability and anti-peak-load regulation, the power from these renewable energy sources cannot be integrated well into the electric grid, resulting in substantial waste and further development restrictions [2].

Employing intermittent renewable electricity to power the reduction of $CO_2$ to fuels is a new transformative energy and negative carbon technology that cannot only reduce $CO_2$ emissions through the utilization of $CO_2$ as feedstock but can also store renewable energy as fuel. Powered by renewable electricity, $CO_2$ can be reduced to various synthetic fuels such as CO, HCOOH, $CH_3OH$, $C_2H_5OH$, and $C_2H_4$. These renewable synthetic fuels can be consumed for power transportation directly or to produce other fuels via the Fischer-Tropsch synthesis process to reduce our dependency on fossil fuels, and the released $CO_2$ can be recycled to form a carbon-neutrality cycle (Fig. 1).

In contrast to thermal catalysis under harsh conditions, electrocatalytic $CO_2$ reduction can be performed at room temperature and atmospheric pressure with a low energy demand and facility requirement, which makes it economically viable for practical applications. More importantly, the reaction of $CO_2$ electroreduction under ambient conditions is highly controllable with a well-defined electroactive component, and the products vary and depend on distinct active sites with different potentials. By employing $CO_2$ electroreduction technology, renewable synthetic fuels, such as CO [3–5] and HCOOH [6–8], have been selectively synthesized with Faradaic efficiencies usually above 90%, and the current densities related to the conversion rate need improvement. The production of multi-carbon renewable fuels, such as ethylene, ethanol, and acetate, is much inferior in terms of selectivity and activity and is currently being improved by regulating catalysts and electrolytic systems.

Although impressive progress has been made, the low $CO_2$ solubility in aqueous electrolytes (34 mmol/L at 25°C and 1 atm) [9] and long mass transfer distance hinder $CO_2$ mass transport, resulting in a very limited current density of tens of mA/cm$^2$ [10–13], which is far below the requirement for industrial applications. One strategy for addressing this issue is to construct gas-diffusion electrodes (GDEs) by coating highly active catalysts on microporous layers decorated with superhydrophobic polytetrafluoroethylene and conductive carbon particles [14–17]. Such GDEs integrated with flow cells or membrane electrode assemblies could promote the rapid diffusion of $CO_2$ to the active sites, thus enabling the reaction to operate at an industrial-scale current density ($\geqslant$ 200 mA/cm$^2$) [18–22]. However, in this system, $CO_2$ inevitably reacts with $OH^-$ to generate carbonate/bicarbonate species that can block the mass transfer channels, and GDEs must also provide sufficient

Received Aug. 15, 2022; accepted Sept. 15, 2022; online Oct. 15, 2022

Yanfang SONG, Xiao DONG, Wei CHEN (✉), Wei WEI (✉)
Low-Carbon Conversion Science and Engineering Center, Shanghai Advanced Research Institute, Chinese Academy of Sciences, Shanghai 201210, China; University of Chinese Academy of Sciences, Beijing 100049, China
E-mails: chenw@sari.ac.cn (Wei CHEN);
weiwei@sari.ac.cn (Wei WEI)

hydrophobicity to prevent frequent flooding [23,24]. Furthermore, the integrated polymer binder may age and loosen during long-term electrolysis, which deteriorates the stability and performance. All of these imperfections limit the potential of GDE systems for industrial applications. Therefore, designing and constructing a new type of functional electrode configuration is essential for achieving excellent selectivity and stability for $CO_2$ electroreduction at an industrial-scale current density.

A three-dimensional hollow fiber porous material with a compact structure can serve as a self-supported electrode without any additives and exhibits promising potential for efficient and high-rate $CO_2$ electroreduction due to enhanced mass transport. The self-supported hollow fiber electrode fabricated by a facile and scalable method (Fig. 2) consisted of only a single active component with an abundant surface area and tunable pore structure. The rich hierarchical porous structure of the hollow fibers provided convenient mass transfer channels for $CO_2$ electroreduction reactions (Fig. 3(a)). With the end of the hollow fiber sealed, gaseous $CO_2$ can be forced to penetrate the porous channels to make good contact with the catalyst and electrolyte, promoting $CO_2$ electroreduction at the gas-catalyst-liquid three-phase boundary. This type of electrode configuration is termed "gas penetration electrode (GPE)" and with its greatly enhanced mass transfer ability, it displays substantial potential in $CO_2$ electroreduction for industrial applications.

Research on hollow-fiber GPEs for synthesizing

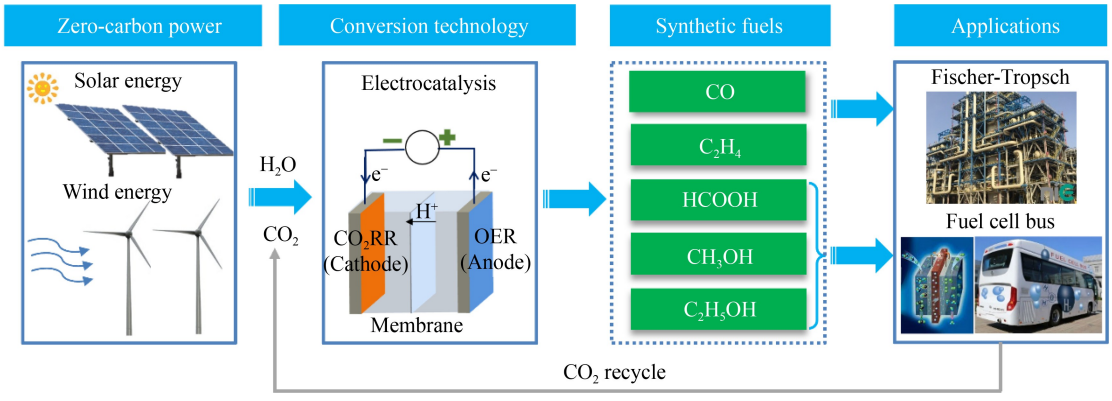


**Fig. 1** Roadmap of renewable fuel production and the carbon cycle via electrocatalytic $CO_2$ reduction powered by renewable energy.

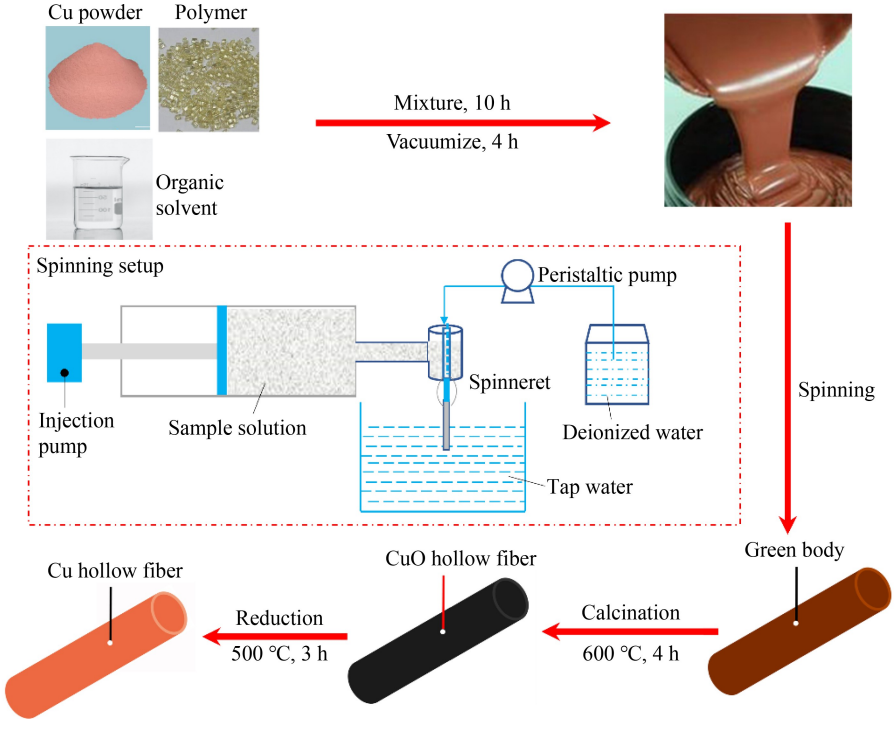


**Fig. 2** Schematic illustration of the preparation of Cu hollow fibers using the coextrusion/coaxial spinning method.

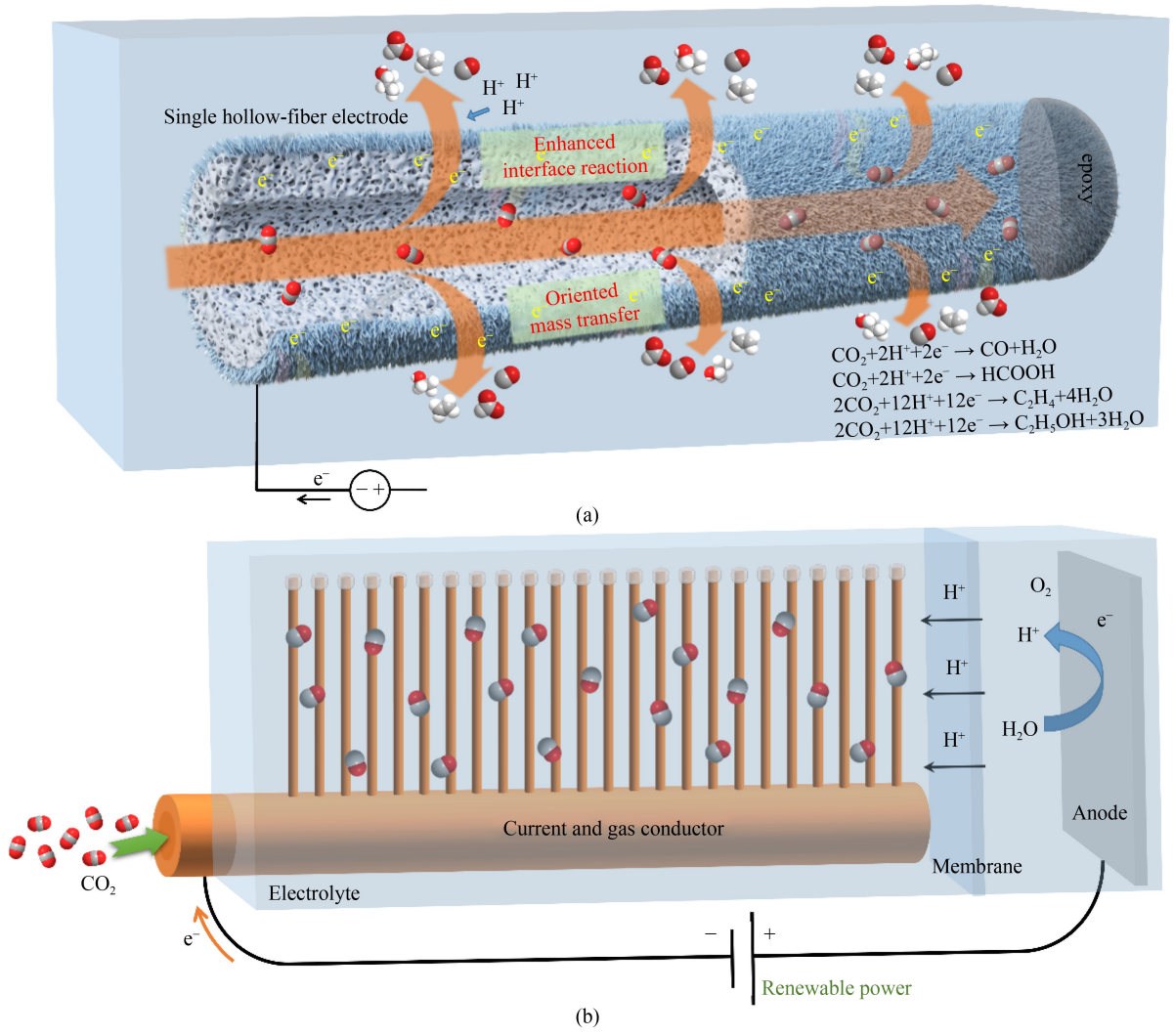


**Fig. 3** Schematic illustrations of hollow fiber gas penetration electrodes.

(a) The hollow fiber electrode with a hierarchical micro/nanostructure for $CO_2$ electroreduction to various products; (b) the large-scale $CO_2$ electroreduction engineering on basis of the hollow fiber array.

renewable fuels has been increasing, and the huge advantages of hollow-fiber GPEs have already been reported. Kas et al. obtained CO yields at least one order of magnitude higher using Cu hollow fibers for $CO_2$ electroreduction compared to nanocrystalline Cu electrodes [25]. Subsequently, Chen et al. constructed freestanding Cu-Sn alloy hollow fibers for selective formate formation from $CO_2$ electroreduction with a Faradaic efficiency of 91% by suppressing hydrogen evolution [26]. Additionally, Yuan et al. adopted an electrodeposition method to decorate Cu hollow fibers with controlled Sn [27,28] or Bi [29] surfaces. The highly rough surfaces provide more catalytically active sites for $CO_2$ electroreduction, resulting in a higher formate partial current density, outperforming other Cu-based GDEs. However, these hollow fiber electrodes have not been working to their full penetrating effect and thus deliver very limited current densities ($\leqslant$ 200 mA/cm$^2$), which is insufficient to afford economically viable $CO_2$ electrochemical conversion.

Recently, our group fabricated Cu hollow fiber GPEs using a phase-inversion/sintering method (Fig. 2), which can stably synthesize formate from $CO_2$ electroreduction at a high current density of 210 mA/cm$^2$ with yields of approximately 16 and 30 times those of Cu foam and Cu foil, respectively [30]. We also fabricated a hierarchical-micro/nanostructured hollow fiber electrode composed of only metallic Ag for $CO_2$ electroreduction, which achieved the efficient formation of CO at ampere-level current density (> 1 A/cm$^2$) [31]. Surprisingly, the $CO_2$ conversion rate on this Ag hollow fiber GPE exceeded 50% at a high space velocity of 31000 mL/($g_{cat}$·h) under ambient conditions. The large current densities (~1.26 A/cm$^2$) and high CO Faradaic efficiencies (~93%) remained quite stable in a continuous test for a long lifespan. Hollow fiber GPEs with an enhanced and

oriented mass transfer function enable the continuous transport of $CO_2$ to the catalyst surface and promote the generation of a three-phase interface between gaseous $CO_2$, the electrode, and the electrolyte, thus achieving an ultrahigh current density, outperforming state-of-the-art hollow-fiber electrodes (Table 1). These insightful studies confirmed that hollow-fiber GPEs exhibit compelling performance for stable $CO_2$ electroreduction at industrial-scale current densities.

Hollow fibers are generally fabricated using the coextrusion/coaxial spinning method with a phase inversion and sintering process [26–33] (Fig. 2). The spinneret used in this method consisted of at least two coaxial tubes. The core solution, normally water, is injected into the central tube to form the hollow fiber. Meanwhile, the sample solution, including the target material, polymer, and organic solvent mixed by ball milling, is excluded from the other tube to generate the shell of the hollow fiber. The shell of the hollow fiber is solidified by inverting the organic solvent with an inorganic solution. The removal of the polymer and final sintering gives rise to a mechanically strong hollow fiber with a finger-like porous structure on the shell. Such a method can be used to fabricate hollow fibers continuously with high flux and uniform structures, making it facile and compatible with existing large-scale production processes. More importantly, the inner and outer diameters of the hollow fibers can be easily adjusted by tuning the flow rate of the core and shell solutions or the diameter of the spinneret, respectively, to optimize the three-phase interface reaction kinetics of $CO_2$ electroreduction. Moreover, the hollow fiber electrode configuration can be expanded from one-layered to multilayered hollow fibers and from one-component to multicomponent hollow fibers to achieve synergistic electrocatalytic $CO_2$ reduction, which may significantly promote the formation of multicarbon renewable synthetic fuels.

The hollow fiber configuration is suitable for large-scale applications because of its high surface/volume-specific ratio, controllable fabrication process, low cost, and suitability for industrial modules. In particular, the higher surface/volume ratio enables hollow fibers to be easily assembled and scaled up. That is, the single hollow fiber on the working electrode can be expanded to an array of multiple well-arranged hollow fibers (Fig. 3(b)), making it viable to scale up $CO_2$ electroreduction to renewable synthetic fuels. Therefore, the electrode area can be enlarged from a few square centimeters at the laboratory level to thousands of square centimeters at the industrial level. Accordingly, the electrode arrangement and layout of the electrolytic cell must be optimized to meet the amplification requirements of the electronic, gas, and electrolyte flow paths. That is, the hollow fiber array arrangement, including the spacing, length, amount, and size of the current conductor and the electrolytic cell, must be compatible with each other, which is a great challenge. The rules of electrode amplification and electrolysis cell design are underway to construct a perfectly suited electrolyzer to overcome the most critical bottleneck in engineering amplification of electrocatalytic $CO_2$ reduction. In addition, metal selection for producing target renewable fuels, construction of hierarchical micro/nanostructures on hollow fibers for enhancing mass transfer, and a thorough investigation of the reaction mechanism and the kinetic process of $CO_2$ electroreduction should be focused upon in future research.

The electrocatalytic $CO_2$ reduction route for producing renewable synthetic fuels using hollow-fiber gas penetration electrodes has huge market potential. In the future, an energy system will be established using renewable energy as the main body. Hollow-fiber integrated electrolytic units powered by zero-carbon electricity are feasible for producing renewable synthetic fuels from $CO_2$ and water. Large-scale synthesized renewable fuels, such as syngas with controllable ratios, can be combined with the Fischer-Tropsch synthesis process to produce long-chain hydrocarbons and other fuels [34]. The released $CO_2$ from the consumption of these fuels can be recycled to form a negative carbon cycle. The advantages of high power output, low fabrication costs, and easy engineering amplification of hollow-fiber gas penetration electrodes make them potentially promising for industrial applications. In addition to the electrocatalytic $CO_2$ reduction route,

**Table 1** Performance comparison of $CO_2$ electroreduction on the current hollow-fiber electrodes

| Catalysts | Electrolyte | Potential/(V vs. RHE) | Products | $J_{total}$/(mA·cm$^{-2}$) | FE/% | Ref. |
|---|---|---|---|---|---|---|
| Cu hollow fiber | 0.5 mol/L $KHCO_3$ | −1.1 | Formate | 210 | 80 | [30] |
| Activated Ag hollow fiber | 0.5 mol/L $KHCO_3$ | −0.83 | CO | 1262 | 93 | [31] |
| Cu hollow fiber | 0.3 mol/L $KHCO_3$ | −0.4 | CO | ~10 | 72 | [25] |
| Cu-$Sn_{45\%}$ hollow fiber | 0.5 mol/L $KHCO_3$ | −0.75 | Formate | 66 | 91 | [26] |
| Cu-Sn hollow fiber | 0.5 mol/L $KHCO_3$ | −1.2 | Formate | 88 | 78 | [27] |
| $Cu_6Sn_5$ hollow fiber | 0.5 mol/L $KHCO_3$ | −1.1 | Formate | 136 | 89 | [28] |
| $CuBi_2O_3$ hollow fiber | 0.5 mol/L $KHCO_3$ | −1.0 | Formate | 141 | 85 | [29] |

hollow-fiber gas penetration electrodes that efficiently produce renewable synthetic fuels can also be achieved through the routes of photoelectrocatalytic $CO_2$ reduction, electrocatalytic $CH_4$ oxidation, photoelectrocatalytic $CH_4$ oxidation, and electrocatalytic $N_2$ reduction. These are also promising for industrial applications, even though they are still in the early stages.

**Acknowledgments** This work was financially supported by the National Natural Science Foundation of China (Nos. 91745114 and 21802160), the "Transformational Technologies for Clean Energy and Demonstration," the Strategic Priority Research Program of the Chinese Academy of Sciences (No. XDA 21000000), Hundred Talents Program of the Chinese Academy of Sciences (No. 2060299), Youth Innovation Promotion Association of the Chinese Academy of Sciences (No. E224301401), Shanghai Sailing Program (No. 18YF1425700), Shanghai Functional Platform for Innovation Low-Carbon Technology, and the Major Project of the Science and Technology Department of Inner Mongolia (No. 2021ZD0020).

## References

1. National Energy Administration of China. The development of renewable energy reached a new level in 2021. 2022–01–28, available at National Energy Administration website
2. National Energy Administration of China. New energy consumption capacity. 2022–06–10, available at National Energy Administration website
3. Won D H, Shin H, Koh J, et al. Highly efficient, selective, and stable $CO_2$ electroreduction on a hexagonal Zn catalyst. Angewandte Chemie International Edition, 2016, 55(32): 9297–9300
4. Ma M, Trzesniewski B J, Xie J, et al. Selective and efficient reduction of carbon dioxide to carbon monoxide on oxide-derived nanostructured silver electrocatalysts. Angewandte Chemie International Edition, 2016, 55(33): 9748–9752
5. Liu M, Pang Y, Zhang B, et al. Enhanced electrocatalytic $CO_2$ reduction via field-induced reagent concentration. Nature, 2016, 537(7620): 382–386
6. Gao S, Jiao X, Sun Z, et al. Ultrathin $Co_3O_4$ layers realizing optimized $CO_2$ electroreduction to formate. Angewandte Chemie International Edition, 2016, 55(2): 698–702
7. Wang Y, Zhou J, Lv W, et al. Electrochemical reduction of $CO_2$ to formate catalyzed by electroplated tin coating on copper foam. Applied Surface Science, 2016, 362: 394–398
8. Zheng X, De Luna P, García de Arquer F P, et al. Sulfur-modulated tin sites enable highly selective electrochemical reduction of $CO_2$ to formate. Joule, 2017, 1(4): 794–805
9. Ross M B, De Luna P, Li Y, et al. Designing materials for electrochemical carbon dioxide recycling. Nature Catalysis, 2019, 2(8): 648–658
10. Zhao C, Wang J. Electrochemical reduction of $CO_2$ to formate in aqueous solution using electro-deposited Sn catalysts. Chemical Engineering Journal, 2016, 293: 161–170
11. Ma M, Liu K, Shen J, et al. *In situ* fabrication and reactivation of highly selective and stable Ag catalysts for electrochemical $CO_2$ conversion. ACS Energy Letters, 2018, 3(6): 1301–1306
12. Zhao C, Dai X, Yao T, et al. Ionic exchange of metal-organic frameworks to access single nickel sites for efficient electroreduction of $CO_2$. Journal of the American Chemical Society, 2017, 139(24): 8078–8081
13. Choi J, Kim J, Wagner P, et al. Energy efficient electrochemical reduction of $CO_2$ to CO using a three-dimensional porphyrin/graphene hydrogel. Energy & Environmental Science, 2019, 12(2): 747–755
14. Lv J J, Jouny M, Luc W, et al. A highly porous copper electrocatalyst for carbon dioxide reduction. Advanced Materials, 2018, 30(49): 1803111
15. Dinh C T, Burdyny T, Kibria M G, et al. $CO_2$ electroreduction to ethylene via hydroxide-mediated copper catalysis at an abrupt interface. Science, 2018, 360(6390): 783–787
16. Ma W, Xie S, Liu T, et al. Electrocatalytic reduction of $CO_2$ to ethylene and ethanol through hydrogen-assisted C–C coupling over fluorine-modified copper. Nature Catalysis, 2020, 3(6): 478–487
17. Dinh C T, García de Arquer F P, Sinton D, et al. High rate, selective, and stable electroreduction of $CO_2$ to CO in basic and neutral media. ACS Energy Letters, 2018, 3(11): 2835–2840
18. Huang J E, Li F, Ozden A, et al. $CO_2$ electrolysis to multicarbon products in strong acid. Science, 2021, 372(6546): 1074–1078
19. Chen C, Li Y, Yu S, et al. Cu-Ag tandem catalysts for high-rate $CO_2$ electrolysis toward multicarbons. Joule, 2020, 4(8): 1688–1699
20. Möller T, Ngo Thanh T, Wang X, et al. The product selectivity zones in gas diffusion electrodes during the electrocatalytic reduction of $CO_2$. Energy & Environmental Science, 2021, 14(11): 5995–6006
21. Peng C, Luo G, Xu Z, et al. Lithiation-enabled high-eensity nitrogen vacancies electrocatalyze $CO_2$ to $C_2$ products. Advanced Materials, 2021, 33(40): 2103150
22. Yang P P, Zhang X L, Gao F Y, et al. Protecting copper oxidation state via intermediate confinement for selective $CO_2$ electroreduction to $C_{2+}$ fuels. Journal of the American Chemical Society, 2020, 142(13): 6400–6408
23. Li H, Liu T, Wei P, et al. High-rate $CO_2$ electroreduction to $C_{2+}$ products over a copper-copper iodide catalyst. Angewandte Chemie International Edition, 2021, 60(26): 14329–14333
24. Zhang X, Li J, Li Y Y, et al. Selective and high current $CO_2$ electro-reduction to multicarbon products in near-neutral KCl electrolytes. Journal of the American Chemical Society, 2021, 143(8): 3245–3255
25. Kas R, Hummadi K K, Kortlever R, et al. Three-dimensional porous hollow fibre copper electrodes for efficient and high-rate electrochemical carbon dioxide reduction. Nature Communications, 2016, 7(1): 10748
26. Chen B, Xu J, Zou J, et al. Formate-selective $CO_2$ electrochemical reduction with a hydrogen-reduction-suppressing bronze alloy hollow fiber electrode. ChemSusChem, 2020, 13(24): 6594–6601
27. Rabiee H, Zhang X, Ge L, et al. Tuning the product selectivity of the Cu hollow fiber gas diffusion electrode for efficient $CO_2$ reduction to formate by controlled surface Sn electrodeposition. ACS Applied Materials & Interfaces, 2020, 12(19): 21670–21681
28. Rabiee H, Ge L, Zhang X, et al. Stand-alone asymmetric hollow

fiber gas-diffusion electrodes with distinguished bronze phases for high-efficiency $CO_2$ electrochemical reduction. Applied Catalysis B: Environmental, 2021, 298: 120538

29. Rabiee H, Ge L, Zhang X, et al. Shape-tuned electrodeposition of bismuth-based nanosheets on flow-through hollow fiber gas diffusion electrode for high-efficiency $CO_2$ reduction to formate. Applied Catalysis B: Environmental, 2021, 286: 119945
30. Zhu C, Shen G, Chen W, et al. Copper hollow fiber electrode for efficient $CO_2$ electroreduction. Journal of Power Sources, 2021, 495: 229814
31. Li S, Chen W, Dong X, et al. Hierarchical micro/nanostructured silver hollow fiber boosts electroreduction of carbon dioxide. Nature Communications, 2022, 13(1): 3080
32. Chen W, Chen S, Liang T, et al. High-flux water desalination with interfacial salt sieving effect in nanoporous carbon composite membranes. Nature Nanotechnology, 2018, 13(4): 345–350
33. Lei L, Pan F, Lindbrathen A, et al. Carbon hollow fiber membranes for a molecular sieve with precise-cutoff ultramicropores for superior hydrogen separation. Nature Communications, 2021, 12(1): 268
34. Huang Z, Zhu L, Li A, et al. Renewable synthetic fuel: turning carbon dioxide back into fuel. Frontiers in Energy, 2022, 16(2): 145–149